Chapter 6

Peristaltic Transport in an Elastic Tube under the Influence of Dilating Forcing Amplitudes: Application to oesophageal swallowing

6.1 Introduction

Elastic property of a material is its ability to oppose a deforming force, which is quite natural. It retains its original shape immediately after the force is removed. Study of viscous flow in elastic tubes is a requirement for learning the true mechanisms of various phenomena (e.g., atherosclerosis, artery replacement by a graft, bolus transport in oesophagus, etc.) in medicine, biology, biomedical technology and also in industry. The information on the mechanisms of oesophageal and intestinal transport of food and liquids is of immense importance for the treatment of patients suffering from transport disorders. The physiology is complex and not fully understood. Models on biological ducts require inclusion of the solid mechanics of the tube wall, the muscle action, material stiffness etc. The tube mechanics should include the shape of the deformable boundary for appropriate modeling. Investigation of peristalsis in elastic tubes is also expected to provide useful information for designing of prosthetic limbs.

On the other hand, introduction of the elastic property of the tube wall makes modeling quite involved in view of solution. The literature treating this problem is focused generally on the dynamics of the ureter (Fung, 1971; Griffiths, 1989; Carew & Pedley, 1997) and flow through blood vessels (Rubinow and Keller, 1972; Vajravelu et al., 2011). The

vascular system comprises a complex configuration of branched elastic tubes. Young (1808) initiated estimation of the significance of elasticity for the pulse wave originating from the heart. Rubinow and Keller (1972) and Fung (1997) considered the Poiseuille's flow locally, and found that the radius of a tube can be determined by the balance between the transmural pressure (i.e. the difference between the inside and outside pressure) and the tension in the tube wall. Takagi and Balmforth (2011) modeled tube wall deformation using linear elasticity and the internal flow assuming the lubrication approximation. Waters and Guiot (2001) investigated flow in an elastic tube subject to a prescribed force. They considered blood homogeneous and Newtonian and the vein an isotropic thin walled elastic tube. Sochi (2014) investigated the flow of Newtonian and power law fluids in elastic tubes considering the lubrication approximation theory. He demonstrated qualitative similarity in general and asymptotic reduction of the flow equations to limiting cases. Uddin et al., (2018) investigated peristaltic transport of a nano-fluid via elastic sheets.

Selvi et al. (2018) analysed the flow of blood in elastic arteries by considering blood as a power-law fluid. Pulsatile flow of a conducting Jeffrey fluid through a porous elastic tube with variable cross section was investigated by Selvi and Srinivas (2018). An analysis was carried out to study magnetohydrodynamics peristaltic flow of Prandtl fluid in a channel with flexible walls by Hayat et al. (2018). Decreasing behaviour of Prandtl fluid parameters on the axial velocity, temperature and heat transfer coefficient was observed. Although the literature on peristalsis is recently flooded with numerous contributions dealing with various aspects such as type of the fluid, electro-conductivity, slip effects etc. but that of the more genuine aspect of elastic property of the vessel is quite scares.

We focus on modeling of bolus transport in oesophagus of the human body. Oesophageal diseases such as oesophageal cancer, Barrett's oesophagus, oesophageal motility disorders, put the human health in danger in the modern society. The study of bolus transport in oesophagus may help cure these diseases. Several authors, including Li and Brasseur (1993), Misra and Pandey (2001), Misra and Maiti (2012), have done considerable amount of work in the past on the transport of food bolus in the oesophagus with different types of geometry for both Newtonian and non-Newtonian fluids. Pandey et al. (2017) discovered dilation of wave amplitude to increase pressure in the distal end of oesophagus. The concept was used to correct flow models for non-Newtonian oesophageal flows (Pandey

and Tiwari, 2017; Pandey et al. 2018). Pandey and Singh (2018a) investigated influence of suspended particle in oesophageal swallowing. Pandey and Singh (2018b) further used this to investigate oesophageal flow affected by hiatus hernia. However, none of them considered the elastic property of oesophageal wall. The review of existing literature reveals that it is highly desirable to have flow models with elastic property of oesophageal wall. A model of oesophageal wall muscle mechanics during bolus transport has been presented by Nicosia and Brasseur (2002). The objective of this work is focused on deformation of a linear elastic oesophageal wall and the flow therein. The tube is assumed to follow a simple constitutive equation, linearly relating the diameter of the tube to the pressure difference between inside and outside the tube.

6.2 Mathematical Formulation

6.2.1 Dimensional equations

We consider oesophagus as an axisymmetric tube described by the cylindrical polar coordinate system (r, x) and filled with an incompressible Newtonian fluid of density ρ, dynamic viscosity μ, internal pressure $p(r, x, t)$ and the velocity field (v, u). We model the oesophageal tube as a linearly elastic, incompressible and isotropic material along which unsteady peristaltic waves move. An inward radial force $F(x - ct) = \epsilon e^{kx} f\left(\frac{x-ct}{\lambda}\right)$ with increasing forcing amplitude ϵe^{kx}, per unit area, is prescribed on the boundary to reflect the elastic property of the tube wall, where k, f, c and λ are respectively amplitude dilation parameter, a dimensionless function that characterizes the spatial structure of the forcing, wave propagation speed and the wavelength. $h(x, t)$ is assumed to be the radial position of wall from center line due to the application of inward radial force F (Fig. 6.1).

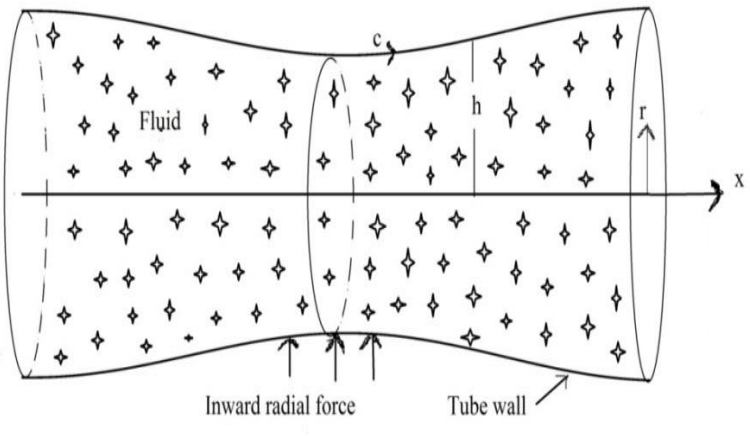

Fig. 6.1 *Schematic diagram of wall position showing inward radial force with dilating forcing amplitude.*

During bolus transport in oesophagus there is a difference of pressures between the inside and the outside of the tubular wall, which may cause the tube to contract or relax. This contraction or relaxation of the tube is due to the elastic property of the wall. The elastic properties of the tube are assumed to cause the transmural pressure difference of the form $p(h,x,t) - p_0 = D\lambda^n \frac{d^n}{dx^n}(h-a) + F(x-ct)$, where $n = 0$ or 4 characterises the type of elastic material constituting the tube, D denotes its stiffness parameter, p_0 is the ambient pressure and a is the equilibrium tube radius attained in its un-deformed state (Takagi and Balmforth, 2011). The case $n = 0$ corresponds to a linearly elastic tube with its deformation proportional to the net radial force while $n = 4$ corresponds to a thin shell of bending stiffness $D = \frac{l^3 E}{12(1-\vartheta^2)}$, where E, l and ϑ denote respectively the Young modulus, shell thickness and the Poisson ratio (Love, 1893). Therefore the force balance on the linearly elastic tube may be written as

$$p(h,x,t) - p_0 = D(h-a) + F(x-ct). \tag{6.1}$$

The Navier-Stokes equations of fluid motion due to the assumption made above are

$$\rho\left(\frac{\partial}{\partial t} + u\frac{\partial}{\partial x} + v\frac{\partial}{\partial r}\right)u = -\frac{\partial p}{\partial x} + \mu\left(\frac{1}{r}\frac{\partial}{\partial r} + \frac{\partial^2}{\partial r^2} + \frac{\partial^2}{\partial x^2}\right)u, \tag{6.2}$$

$$\rho\left(\frac{\partial}{\partial t}+u\frac{\partial}{\partial x}+v\frac{\partial}{\partial r}\right)v=-F-\frac{\partial p}{\partial r}+\mu\left(\frac{1}{r}\frac{\partial}{\partial r}+\frac{\partial^2}{\partial r^2}+\frac{\partial^2}{\partial x^2}-\frac{1}{r^2}\right)v\,, \tag{6.3}$$

Equation of continuity is

$$\frac{\partial u}{\partial x}+\frac{1}{r}\frac{\partial(rv)}{\partial r}=0\,. \tag{6.4}$$

6.2.2 Boundary conditions

For the boundary conditions, we consider no-slip between the fluid and the tube wall, impose regularity along the centerline of the tube and assume that the tube deforms almost radially. Hence,

$$u(r,x)|_{r=h}=0,\quad \left.\frac{\partial u}{\partial r}\right|_{r=0}=0,\quad v(r,x)|_{r=0}=0,\quad v(r,x)|_{r=h}=\frac{\partial h}{\partial t}. \tag{6.5}$$

6.2.3 Dimensionless formulations

We now remove the dimensions by defining the non-dimensional variables as follows:

$$\left.\begin{aligned} &x'=\frac{x}{\lambda}\,,\ \ r'=\frac{r}{a}\,,\ \ t'=\frac{ct}{\lambda}\,,\ \ u'=\frac{u}{c},\quad v'=\frac{v}{c\alpha}\,,\\ &\alpha=\frac{a}{\lambda}\,,\quad h'=\frac{h}{a}\,,\quad k'=k\lambda\,,\ \ \epsilon'=\frac{\epsilon a}{\mu c},\ \ Q'=\frac{Q}{\pi a^2 c}\,,\\ &p'=\frac{(p-p_0)a^2}{\mu c\lambda}\,,\ \ R_e=\frac{\rho c a}{\mu},\ \ \psi'=\frac{\psi}{\pi a^2 c}\,,\quad D'=\frac{Da^3}{\mu c\lambda}\,. \end{aligned}\right\} \tag{6.6}$$

Invoking the above defined non-dimensional parameters in Eqs. (6.1)-(6.5) followed by low Reynolds number and long wavelength approximations and dropping the primes, Eqs. (6.1)-(6.5) reduce respectively to the following dimensionless form:

$$p(h,x,t)=D(h-1)+\epsilon e^{kx}f(x-t), \tag{6.7}$$

$$\frac{\partial p}{\partial x}=\frac{1}{r}\frac{\partial}{\partial r}\left(r\frac{\partial u}{\partial r}\right), \tag{6.8}$$

$$\frac{\partial p}{\partial r}=0, \tag{6.9}$$

$$\frac{\partial u}{\partial x}+\frac{1}{r}\frac{\partial(rv)}{\partial r}=0, \tag{6.10}$$

$$u(r,x)|_{r=h} = 0, \quad \left.\frac{\partial u}{\partial r}\right|_{r=0} = 0, \quad v(r,x)|_{r=0} = 0, \quad v(r,x)|_{r=h} = \frac{\partial h}{\partial t}. \tag{6.11}$$

6.3 Solution

Integrating Eq. (6.8) with respect to r twice in view of Eq. (6.9) and imposing the first and second boundary conditions of (6.11), the axial velocity is obtained as

$$u(r,x,t) = \frac{1}{4}\frac{\partial p}{\partial x}(r^2 - h^2)\,. \tag{6.12}$$

Integration of Eq. (6.10) with respect to r, by substituting the axial velocity from Eq. (6.12) under the third condition of Eq. (6.11), gives the radial velocity as

$$v(r,x,t) = \frac{r}{4}\left[h\frac{\partial h}{\partial x}\frac{\partial p}{\partial x} - \frac{1}{4}\frac{\partial^2 p}{\partial x^2}(r^2 - 2h^2)\right]. \tag{6.13}$$

We opt for the following transformations from the laboratory frame (r,x) to the wave frame (R,X) in order to find volume flow rate in the wave frame:

$$\left.\begin{array}{l} X = x - t, \quad U(R,X) = u(r,x,t) - 1, \quad V(R,X) = v(r,x,t), \\ H(X) = h(x,t), \qquad P(X) = p(x,t), \qquad q = Q - h^2\ . \end{array}\right\} \tag{6.14}$$

Volume flow rate in the wave frame is $q = 2\int_0^H URdR$ which, in view of the transformations (6.14) and Eq. (6.7), gives

$$q = -H^2 - \frac{H^4}{8}\left[D\frac{dH}{dX} + \epsilon\frac{d(e^{kX}f(X))}{dX}\right]. \tag{6.15}$$

For small amplitude radial forcing, $\epsilon \ll 1$. Hence, the change in radius due to the application of radial force may be solved using a regular perturbation expansion

$$H = 1 + \epsilon H_1 + \epsilon^2 H_2 + \ \ldots\ldots\ldots\ . \tag{6.16}$$

Inserting the series expansion (6.16) in Eq. (6.15) and collecting the coefficients of ϵ and ϵ^2on the two sides separately, it leads to a set of ordinary differential equations given by

$$D\frac{dH_1}{dX} + 16H_1 = \ -\frac{d(e^{kX}f(X))}{dX}, \tag{6.17}$$

$$D\frac{dH_2}{dX} + 16H_2 = -8{H_1}^2 - 4DH_1\frac{dH_1}{dX} - 4H_1\frac{d(e^{kX}f(X))}{dX} \tag{6.18}$$

Since the homogeneous solutions to Eqs. (6.17) and (6.18) are non-periodic; we take only non-homogeneous solutions for different radial forcing $f(X)$.

6.3.1 Sinusoidal wave forcing

With sinusoidal forcing, $f(X) = sin\,X$, the low amplitude solution to Eqs. (6.17) and (6.18) are

$$H_1 = -\frac{e^{kX}}{c_2}(16\,cos\,X + c_1\,sin\,X),$$

$$H_2 = -\frac{e^{2kX}}{{c_2}^2}(c_3 - c_4\,cos\,2X + c_5\,sin\,2X),$$

where

$$c_1 = D + Dk^2 + 16k, \tag{6.19}$$

$$c_2 = 256 + 32Dk + D^2k^2 + D^2, \tag{6.20}$$

$$c_3 = \frac{2\left(256-8b+{c_1}^2\right)+k\left\{-c_1c_2+D\left(256+{c_1}^2\right)\right\}}{(8+Dk)},$$

$$c_4 = \frac{1}{64+16Dk+D^2k^2+D^2}\left\{-Dc_1(192+c_2) + D^2(-256+{c_1}^2) + 16(-256+8c_2+{c_1}^2) + k^2D\left(-c_1c_2 + D(-256+{c_1}^2)\right) + 2k\left(-4c_1c_2 + 5D(-256+{c_1}^2)\right)\right\},$$

$$c_5 = \frac{2}{64+16Dk+D^2k^2+D^2}\left\{16D^2c_1\left(1+k^2\right) - 4\left(16kc_2 + c_1(c_2-64)\right) + D\left(160kc_1 + 3{c_1}^2 - 768 - 8c_2\left(1+k^2\right)\right)\right\}.$$

Therefore, wall position of the oesophageal tube in the wave frame, up to the second order, is given by

$$H(X) = 1 - \epsilon\frac{e^{kX}}{c_2}(16\,cos\,X + c_1\,sin\,X) - \epsilon^2\frac{e^{2kX}}{{c_2}^2}(c_3 - c_4\,cos\,2X + c_5\,sin\,2X). \tag{6.21}$$

Since the second order term contributes quite less in magnitude, we moderate the solution up to the first order term only for graphical plotting. The wall equation of the oesophageal tube in the laboratory frame, up to the first order may be given by

$$h(x,t) = 1 - \epsilon \frac{e^{kx}}{c_2}\{16cos(x-t) + c_1 sin(x-t)\}. \tag{6.22}$$

Time-averaged volume flow rate: The volume flow rate in the laboratory frame is $Q(x,t) = 2\int_0^h urdr$. Therefore, in view of Eq. (6.12), we get $Q(x,t) = -\frac{1}{8}\frac{\partial p}{\partial x}h^4$.

The time-averaged volume flow rate over a period is $\bar{Q}(x) = \int_0^1 Qdt$ which, on using the transformation (6.14), may be put in the form $\overline{Q(x)} = q + \int_0^1 h^2 dt$, and hence substituting $h(x,t)$ from Eq. (6.22), we obtain

$$\overline{Q(x)} = q + 1 + \epsilon \frac{e^{kx}}{c_2}\{2\,c_1 cos\,x - 2\,c_1 cos(x-1) + 32\,sin(x-1) - 32 sinx\} + \epsilon^2 \frac{e^{2kx}}{{c_2}^2}\Big\{128 + \frac{{c_1}^2}{4}(2 + sin(2x-2) - sin2x) + 8c_1(cos(2x-2) - cos2x) + 64(sin2x - sin(2x-2))\Big\}. \tag{6.23}$$

It may be noted that c_1 and c_2 have already been defined by expressions (6.19) and (6.20).

Stream Function: In the wave frame, steady flow patterns below the peristaltic waves are given by the contours of the constant stream function, Ψ, which are obtained by the solution of the differential equation

$$d\Psi = 2RUdR - 2RVdX. \tag{6.24}$$

Using Eqs. (6.12)-(6.13) under the transformations (6.14), Eq. (6.24) becomes an exact differential equation. Thus the stream function, $\psi(r,x,t)$, in the laboratory frame, is given by

$$\psi(r,x,t) = \frac{r^2}{8}\Big\{D\frac{\partial h}{\partial x} + \epsilon \frac{d(e^{kx}f(x))}{dx}\Big\}(r^2 - 2h^2) - r^2\,. \tag{6.25}$$

6.3.2 Solitary wave with Gaussian forcing

For solitary wave forcing, $f(X) = e^{-\frac{X^2}{2}}$, the solution to Eq. (6.17) may be reduced in terms of the Fourier transform,

$$H_1 = \frac{i}{2\pi}\int_{-\infty}^{\infty} \frac{\omega e^{i\omega X}\bar{f}(\omega)d\omega}{(i\omega)D-16}, \tag{6.26}$$

where $\bar{f}(\omega) = \int_{-\infty}^{\infty} f(X)e^{kX}\, e^{-i\omega X}dX$ denotes the Fourier transform to $f(X)e^{kX}$.

6.4 Results and discussions

Elastic property in tubes, conveying fluids, has been extensively studied in the context of biological and physiological applications during last several years. The objective of the present investigation is to study the fluid mechanics through oesophagus when the elastic wall is prescribed an external inward radial forcing which is assumed to consist of a progressive wave. We mainly study the effect of forcing amplitude of the inward radial force which reflects the elastic property of the oesophageal wall. Pressure, time-averaged volume flow rate and stream function along the axis of the oesophageal tube are determined numerically. The relations of the axial and radial velocities of the fluid versus the radius of the tube are also displayed through graphs. We obtain useful observations for forcing amplitude on pressure, velocities, the time-averaged volume flow rate and stream function.

For the pressure variation along the axis of the tube (Fig. 6.2), we set some parameters such as $D = 1,\ k = 0.02$. For the exploration, we assume that the oesophagus contains three boluses together at a time. The primary concern is the pressure variation along the axis of the oesophagus when a train of boluses travels down the oesophagus towards the distal end. It is observed in Fig. 6.2(a), which corresponds to $t = 0$, that the influence of the forcing amplitude on the pressure variation is to enhance p as ϵ increases from 6 to 8. Moreover, pressure rises at the inlet and then drops to the trough representing pressure at the progressing head of the first bolus, and further rises at the tail of the second bolus. This pattern of pressure distribution repeats up to the distal end of the oesophagus where the final pressure is once again zero but the peak and the trough of the pressure at the distal end is greater than that at the proximal end. This happens due to dilating forcing amplitude which

confirms the observation of Pandey et al. (2017). At $t = \pi$, the boluses are ahead and a part of a new bolus has moved into the oesophagus. This changes the pressure distribution in which pressure goes down at the inlet to pave way for a new bolus.

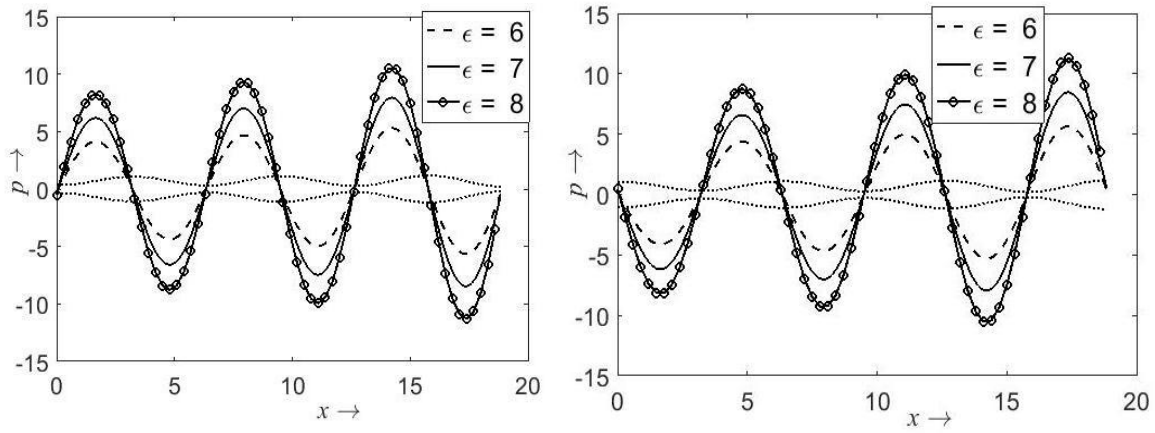

(a) $t = 0.0$ (b) $t = \pi$

Fig. 6.2(a-b) *Pressure versus axis of the tube for different forcing amplitude* $\epsilon = 6, 7, 8$ $(D = 1, k = 0.02)$. *Light dotted lines represent wall position of tube.* (a) $t = 0.0$ *and* (b) $t = \pi$.

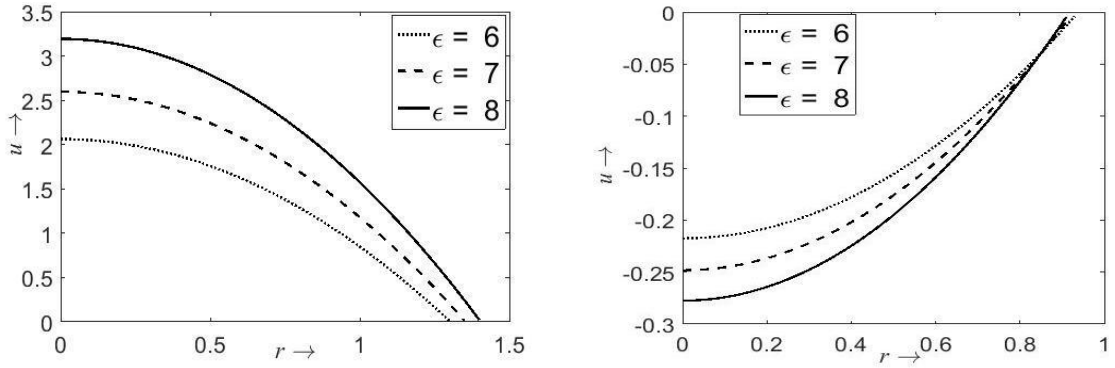

(a) $t = 1.5$ (b) $t = 2.5$

Fig. 6.3(a-b) *Axial velocity of fluid versus radius of the tube at different forcing amplitude* $\epsilon = 6,\ 7,\ 8$ $(D = 1,\ k = 0.02,\ x = 4)$. (a) $t = 1.5$ *and* (b) $t = 2.5$

In Fig. 6.3, we display the impact of forcing amplitude on the axial velocity of the fluid versus the radius of the tube for three different values of forcing amplitudes $\epsilon = 6, 7, 8$ with $D = 1, k = 0.02$ at fixed axial position $x = 3$. Fig. 6.3(a), which corresponds to $t = 1.5$, reveals that the axial velocity increases as the forcing amplitude increases. We also observe in Figs. 6.3(a) and 6.3(b) that the magnitude of the axial velocity is maximum at the axis and zero at the tube wall corresponding to each forcing amplitude. This confirms the no-slip condition at the tube wall. The difference between the axial velocities for two different forcing amplitudes is greater at the radial axis than that in the vicinity of the tube wall.

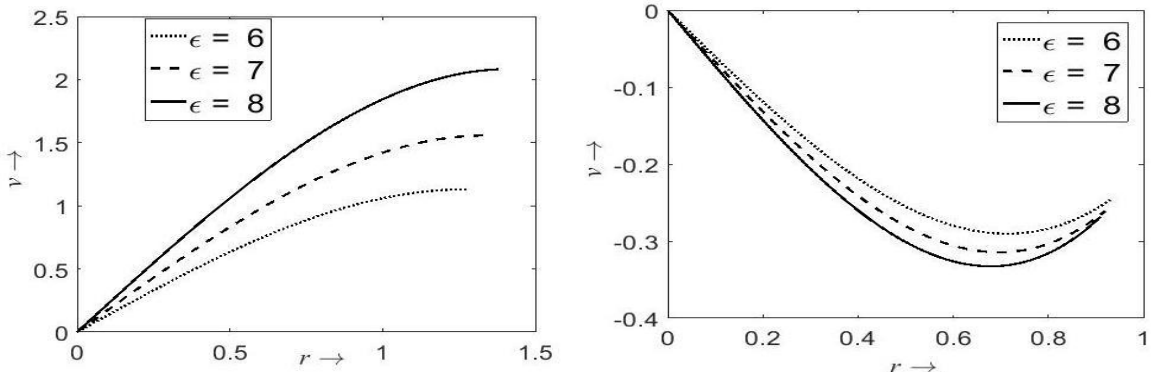

(a) $t = 0.0$ (b) $t = 2.5$.

Fig. 6.4(a-b) *Radial velocity along tube radius showing the impact of forcing amplitude* $\epsilon = 6, 7, 8$ $(D = 1, k = 0.02, x = 4)$. (a) $t = 0.0$ *and* (b) $t = 2.5$.

Figure 6.4 illustrates the impact of the forcing amplitude on the radial velocity of the fluid along the radius of the tube at a specific axial location $x = 4$ for three different values of forcing amplitudes $\epsilon = 6, 7, 8$ with $D = 1$ and $k = 0.02$. Figs. 6.4(a) and 6.4(b) correspond to two distinct time instants $t = 0.0$ and $t = 2.5$ respectively. Analyzing the behaviour of flow in the present figure, we observe that all the curves either rise or fall from zero on the axis as these move away from it and finally attain some finite non-zero value towards the wall surface of the tube. This is to be noted that when the tube relaxes, the radial velocity is positive but once it contract, the direction of motion is reversed and hence the radial velocity becomes negative. This behavioral alteration of the radial velocity along the

radius of the tube confirms the presence of wall motion in the transverse direction. Fig. 6.5 exhibits the relation between the wall position and time. The radial velocity consists of a factor $\partial h/\partial t$, which changes the sign as h increases or decreases with t. It is also observed that the magnitude of the radial velocity increases with increasing forcing amplitude.

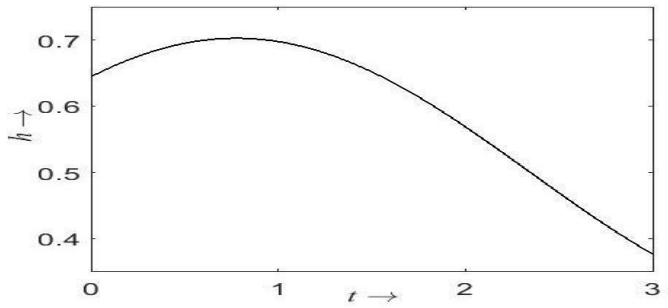

Fig. 6.5 *Wall position versus time at fixed axial position* $x = 4$ $(\epsilon = 6,\ D = 1,\ k = 0.02)$.

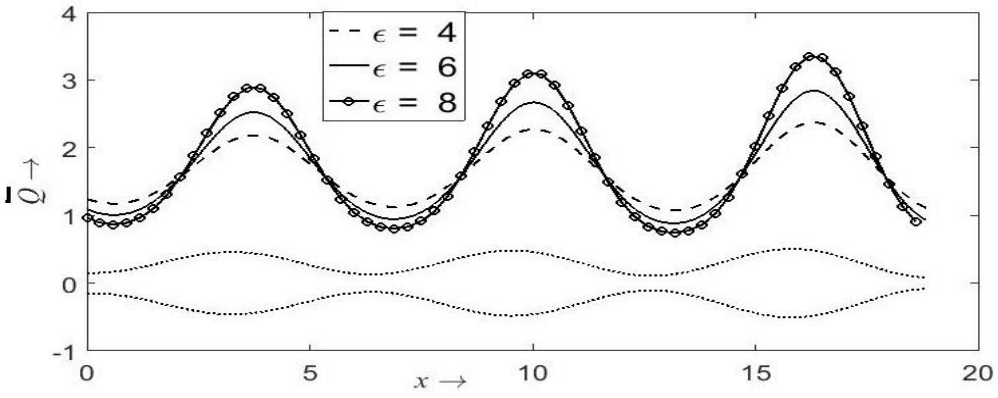

Fig. 6.6 *Time-averaged volume flow rate versus axis of oesophageal tube showing the impact of forcing amplitude* $\epsilon = 4,\ 6,\ 8$ $(q = 0.8,\ D = 1,\ k = 0.02)$. *Light dotted lines represent wall position of oesophageal tube.*

Figure 6.6 presents the variation of the time-averaged volume flow rate $(\bar{Q})$ along the axis of the elastic tube for three different forcing amplitudes $\epsilon = 4,\ 6,\ 8$ with $D = 1$ and $k = 0.02$. It is clear that $\bar{Q}$ increases with the forcing amplitudes whereas an opposite

behaviour is noticed in the contracted region of the tube. It is also observed here that the peak of $\bar{Q}$ near the distal end is higher than that near the proximal end. This happens due to the dilating forcing amplitude.

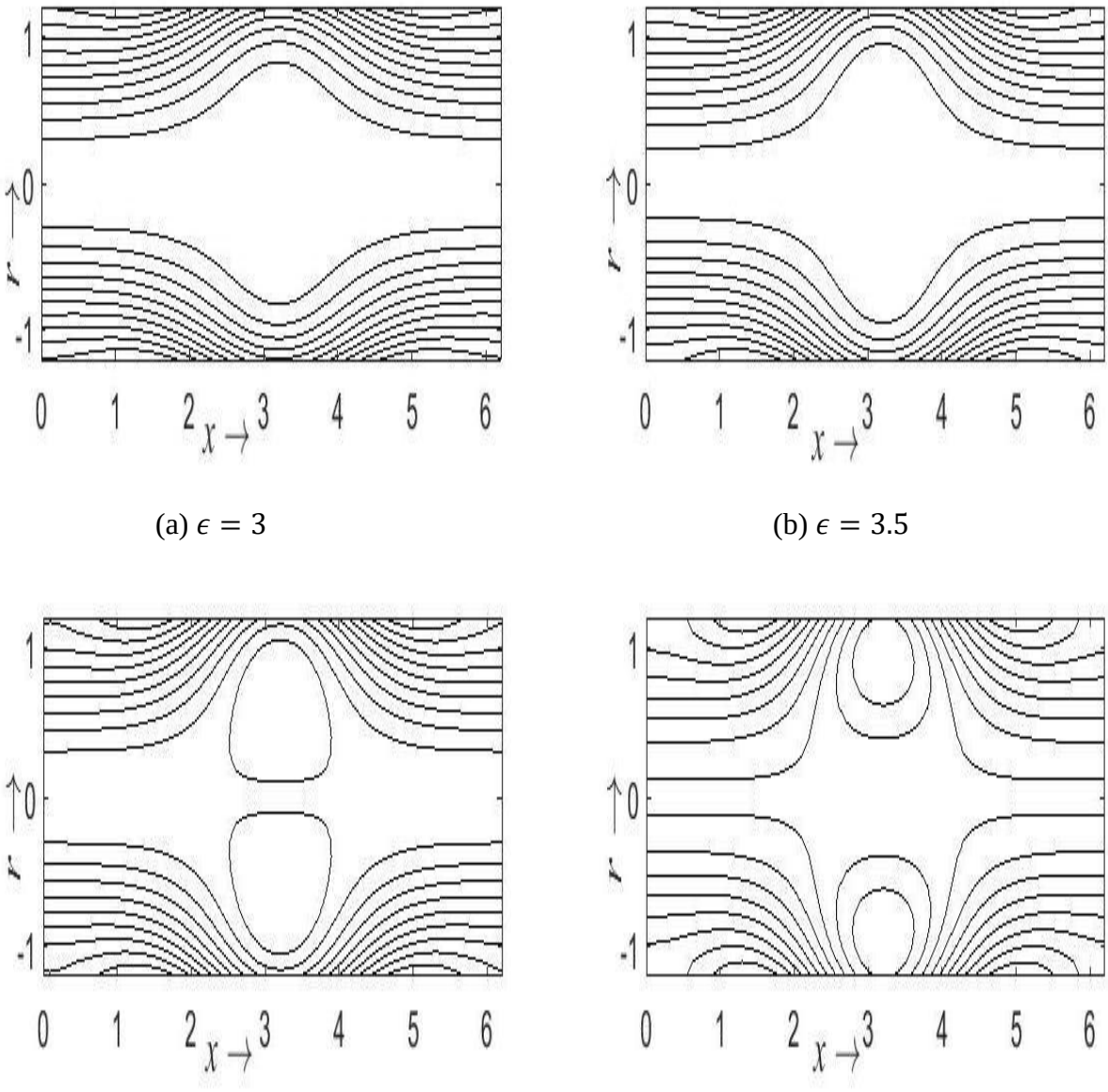

(a) $\epsilon = 3$ (b) $\epsilon = 3.5$

(c) $\epsilon = 4.0$ (d) $\epsilon = 5.0$

Fig. 6.7(a-d) *Stream function showing the impact of forcing amplitude* (a) $\epsilon = 3$, (b) $\epsilon = 3.5$, (c) $\epsilon = 4.0$ (d) $\epsilon = 5.0$ *and others parameters are* $D = 1$ *and* $k = 0.02$.

Streamlines in the laboratory frame with $k = 0.02,\ D = 1,\ t = 0.0$ at different forcing amplitude ($\epsilon = 3\ ,\ 3.5,\ 4.0,\ 5.0$) are shown in Fig. 6.7 which has four parts. A close look of these figures reveal that when ϵ is increased, the streamlines similar to the shape of the tube wall (Fig. 6.7a) change their shape and above a certain ϵ, the central streamlines split to surround a ring-shaped bolus of the fluid (Figs. 6.7c and 6.7d). This ring-shaped bolus of the fluid is now pushed ahead along with the peristaltic wave. This phenomenon is called trapping. Generally, trapping phenomenon occurs at high occlusion and high flow rate.

6.5 Conclusions

Peristaltic transport of food bolus through oesophagus has been investigated theoretically by considering the oesophagus as an elastic tube. The dimensionless radius variation of the tube is determined by perturbation techniques as part of the solution. Impacts of increasing forcing amplitude on pressure, velocities and time averaged volume flow rate are examined and streamline patterns are also drawn. It is observed that the presence of elasticity affect the pressure, pumping performance and velocity significantly. A rise in the forcing amplitude of inward radial force enhances the pressure, time-averaged volume flow rate and hence also the axial and radial velocities. Therefore, we conclude that the elasticity of oesophageal tube favours swallowing of a food bolus.